NEW FRONT. CHEM. (**2018**)
Volume 27, Number 2, pp. 105-113
ISSN 2393-2171; ISSN-L 2393-2171
© West University of Timişoara
Former: Ann. West Univ. Timisoara – Series Chem.
ISSN: 1224-9513

Research Note

TOPOLOGICAL EVOLUTION OF THE 5|8|5 DEFECT IN GRAPHENE

Ottorino ORI (1) and Mihai V. PUTZ (2,3,*)

1. Actinium Chemical Research, Rome, Italy
2. Laboratory of Renewable Energies-Photovoltaics, R&D National Institute for Electrochemistry and Condensed Matter –INCEMC–Timisoara, Timisoara, Romania
3. Laboratory of Structural and Computational Physical-Chemistry for Nanosciences and QSAR, Biology-Chemistry Department, West University of Timisoara, Timisoara, Romania

ABSTRACT

The divacancy 5|8|5 planar defect in graphene show a typical evolution that has been theoretically simulated in this paper by using standard topological modelling techniques. The results point out the ability of the topological roundness in describing complex structures of the graphene plane with several types of polygons. Present considerations, by matching literature findings based on DTF studies,allow a better understanding on the relative stabilityof various defects in graphene and, in particular, therole played by long-range interactions in sp^2 systems.

Keywords: topological efficiency index, topological roundness, 5|8|5 defect, graphene.

1. INTRODUCTION

The mathematical properties of graphenic structures based on their symmetry and topology is an important topic in modern material science. Graphene has in fact attracted expanding technological interest for its unordinary electrical properties like, for example, outstanding ballistic transport properties and longest mean free path at room temperature, distinctive integral and half-integral quantum hall effect and much more [1,2,3]. Graphene - *the miracle material* - has been considered since its discovery made in 2004 by the two Russian-born scientists, Andre Geim and Konstantin Novoselov, both Nobel laureate in 2010, as the ideal candidate material for the next *post-silicon electronics*. Its honeycomb (finite) lattice presents two different types of edges: armchair and zigzag, which largely influence the electronic properties of graphene [4,5]. The main limitation to the applications it is

represented by the *absence of a semiconducting gap in pristine graphene*. The search for industrial methods to create tunable band-gap in graphene poses significant challenges for graphene-based devices, since the introduction of defects showed potential solutions to this important aspect. On one side in fact electronic and mechanical properties of graphene get deteriorated by the presence of structural and topological defects appearing during the lattice growth. On the other side however, deviations from atomic periodicity make it possible to achieve new functionalities. Defects can be introduced into graphene, for example, by irradiation or chemical treatments. The flatness of the graphene sheet mainly descends from the sp^2-hybridized states of the carbon atoms composing the layer. This chemical characteristic allows a cascade of interesting rearrangements of the carbon atoms that may form various type of polygons tiling the graphenic layer, breaking in such a way the perfect hexagonal symmetry of the pristine flat lattice. Many different structures may be created with the usage of non-hexagonal rings, influencing in such a way the local curvature depending from the type of defective (non-hexagonal) polygons that are present. For example, an isolated pentagon induces the formation of a nano-cone but on the contrary, two pentagons connected by an octagon (5|8|5defect) leave the lattice locally flat [6,7].This huge variety of morphological properties is not offered by bulk crystals like diamond or semiconductors that are made by sp^3atoms. Very important to notice that the "reconstructions in the atomic network permit a coherent (topologically) defective lattice without under coordinated atoms" [8] allowing the generation of two classes of defects in the sp^2mesh. We have in fact i) point defects (vacancies or interstitial atoms)that are zero-dimensional and ii) 1D linear defects, each defect showing a certain mobility, exponentially increasing with the temperature, in the graphene plane with defect-specific activation barriers.

In this note, we focus on the *topological evolution* of the 5|8|5defect that has important influences on chemical, electronic, magnetic, and mechanical properties of graphene-based nanodevices. We shall not consider here the mechanisms that lead to the formation of this type of defect because the authors already have devoted a specific work [7] to the topic, proposing an original and fully isomeric mechanism based on the usage of *smart sequences* of Stone-Wales (SW) rearrangements of the pristine hexagonal plane. This isomeric model provides a valid alternative to the 2-vacancy mechanism that is normally invoked in literature [8]to describe the origin of the 5|8|5defective region with an energy barrier of about 8eV, say 4eV per vacant atom. Topological reorganizations of large portion of the graphene lattice have a lower probability of formation (having the standard 5|7|7|5 SW defect a formation energy of about 10eV[9] these rotations present in fact high activation barriers), nevertheless these kinds of mechanisms are important not only from the theoretical pint of view, allowing a much profound understanding about the behaviors of the sp^2 networks in presence of non-hexagonal polygons, but also from practical reasons since ion irradiation or rapid temperature quenching create the conditions that lead to the formation of SW-type rearrangements in fullerenes or graphenic planes, these unfavored routes may play a role in the creation of defects in graphene plane or graphenic regions (i.e. made by hexagons) in large fullerenes [9,10,11].

2. TOPOLOGICAL INVARIANTS

Consider G being a chemical graph with N nodes and B bonds. Distance-based topological invariants have been extensively applied to simulate stability/reactivity of hexagonal systems seen as graphs [12], in which the *chemical distance* d_{vu} is merely the

number of bonds connecting, along the shortest path, the two nodes *v* and *u*, with d_{vv}=0 by definition. With the name Wiener-weight w_v of the node *v* we call the invariant:

$$w_v = \frac{1}{2}\sum_{u=1}^{N} d_{vu} \qquad (1)$$

According with the topological modeling approach, graph invariant (1) represents a powerful atomic descriptor having peculiar prerogatives: a) w_v it is inversely proportional to the *reactivity* of the node b) and inversely proportional to the *compactness* of the graph. The Wiener index *W* of the whole graph is just the sum of the Wiener-weights:

$$W = \sum_{v=1}^{N} w_v \qquad (2)$$

Moreover, $w_v$allows c) the direct *topological measure* of the *topological roundness* of the graph, expressed in this case by the *extreme topological efficiency index*ρ^E:

$$\rho^E = {}^{W}/_{\underline{W}} \; ; \qquad \rho^E \geq 1 \qquad (3)$$

in which $\underline{w} = \min\{w_v\}$ and $\overline{w} = \max\{w_v\}$.The most *compactly-embedded* vertices of G (the so-called *minimal vertices or minimal nodes*) have Wiener-weight equal to $\underline{w}$. Invariant (3) awards the ability of graph nodes to be connected to the other vertices with an efficiency comparable to the one of the minimal vertices; highly efficient graphs like graphene periodic lattice tend therefore to minimize ρ^E, i.e. to have $\rho^E \sim 1$. Topological roundness is considered here to act like a topological potential $\Xi\rho^E = \rho^E$driving the systems toward the "most round" topological configurations by minimizing the ρ^E value. It is worth noticing here that the topological descriptors given by Equations (1-3) are built on the chemical distances d_{vu} connecting *any pairs* of atoms in the system. These descriptors, and in particular the topological potential $\Xi\rho^E$ are in this way able to naturally describe the effects of long-range interactions in sp2 graphene lattices.

This fast and elegant computational model is applied once more in this article to describe the evolution of a defective graphenic lattice with a 5|8|5 defect. The lattice reconstruction process leads to complex modifications of "the electronic charge density and this varies the bond lengths within and around" the 5|8|5 defect [13] preserving the *local flatness* of the defective lattice. This pentagon-octagon-pentagon linear structure, like the one embedded in the 6x4 hexagonal super-cell G_0 represented in Figure 1, maintains the sp^2 hybridization state. The graphene-flake G_0consists in 96 nodes and B=144 bonds if periodic boundary conditions are imposed in both directions (Figure 1a). All the atoms are topologically equivalent $\rho^E(G_0) = 1$with $\underline{w}(G_0) = \overline{w}(G_0)$=260 and $W(G_0)$ =24960.

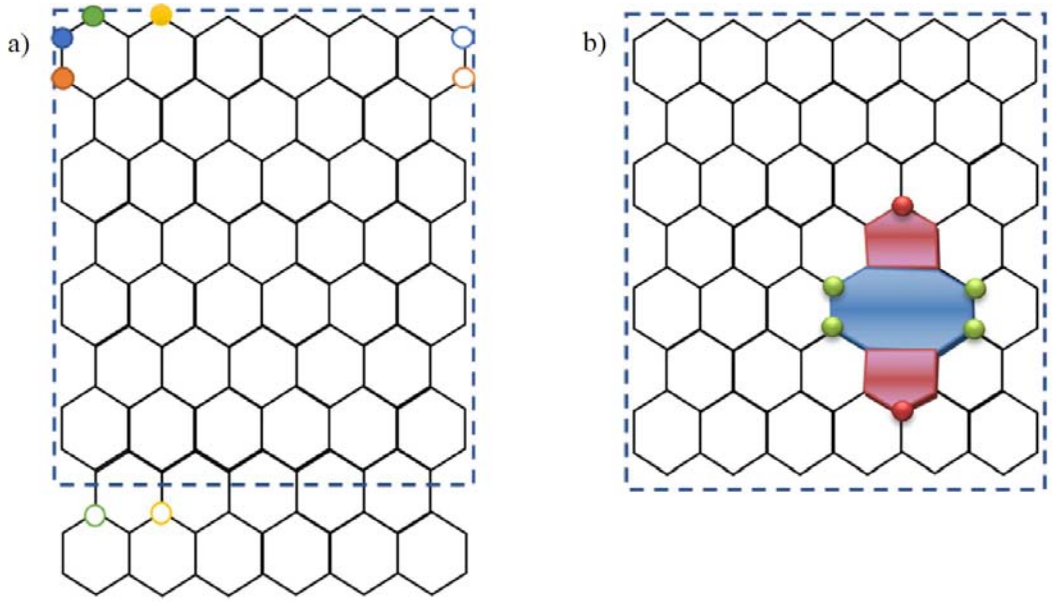

Figure 1.a) The original G_0 6x4 super-cell (dashed rectangle)has 96 atoms with 3 bonds each when the periodic conditions are applied in both directions (solid and circled balls with the same colors are connected by 1 periodic bond). b) The polygons forming the 5|8|5 defect are 2 pentagons (red) and 1 octagon (blue),the remaining hexagons are in white; this periodic super cell G_{585}has 94 nodes still with 3 bonds each.

The polygons forming the 5|8|5 defect are pictured (Figure 1b) in red (pentagons) and blue (octagon) and they are embedded in the hexagons (white) of the pristine graphenic lattice. The defective graphenic system G_{585} shows now 94 nodes (the 5|8|5 defect is generated by a divacancy so G_{585} has two atoms less than G_0) and B=3N/2=141 bonds still under periodic boundary conditions. The presence of the non-hexagonal rings breaks in G_{585} the symmetry of the nodes. Now the minimal nodes are the 4 nodes placed pairwise on the opposite sides of the octagon represented with green balls in Figure 1b. These minimal vertices have $\underline{w}(G_{585})$ =244.5and they represent, in the topological picture, the most stable atoms of the systems. On the other hand, the 2 red balls with $\overline{w}$=256.5 that sit on the pentagons, indicate the two most reactive nodes of G_{585}.The topological roundness passes in this way to the $\rho^B(G_{585}) = 1.04907975$and the Wiener index is W(G_{585}) =23619. The topological efficiency is increased by the presence of the 5|8|5 defect and the fact that $\rho^B(G_{585}) > \rho^B(G_0)$ evidences the energy cost that is necessary to create the divacancy structure. This barrier has been determined to be 8eV, approximately "of the same order of the single vacancy formation "with the evident gain, since two atoms are missing, in the energy permissing atom (4 eV per atom)" [9]. In literature several molecular simulation studies report in fact that two initially isolated vacancies in the graphene layer may coalesce into the 5|8|5 configuration that is the starting point G_{585} of the present research (Figure 1b). The 5|8|5 defect may in fact evolve toward other configurations of the graphenic lattice able to accommodate two missing atoms [9]. These configurations are generated via SW bond rotations and give rise to extended defects that are frequently observed in electron microscopy experiments [17] (see also references articles reported in [9]). The following section is

devoted to study the transformations of the 5|8|5 defect into the two standard configurations one may build via two successive SW flips: the triple pentagon-triple heptagon (555-777) defect and then the quadruple pentagon / hexagon / quadruple heptagon(5555-6-7777) most stable defect [13]. Our computation will be based on the variations of the topological indices induced by the SW rotations on the periodic super-cell made of 94 sp^2 atoms whose starting configurations is represented by G_{888} (see Figure 1 and Figure 2 below).

3. TOPOLOGICAL SIMULATION AND DISCUSSIONS

The first rearrangement of the G_{888} lattice that allows an energy gain of about 0.9 eV [14,15,16] is obtained when one of the 2 side edges of the octagon is rotated with a typical SW rearrangement. In [14] authors also provide a direct evaluation of the energy gap of 0.8 eV still favoring the SW rotation. Recent DFT computations on the same configurations still favor the rotation of the edge of the octagon evidenced in Figure 2a with the arrow, but they reduce the energy gain to 0.53 eV [13].

This SW rotation transforms the 5|8|5 defect into anew arrangement, energetically favored, made of three pentagons and three heptagons (the (555-777) defect) which is normally observed by the experiment study [17].The same defects may be formed on the surface of the carbon nanotubes (CNT's) with an energy gain that depends from the size and from the chirality of the system [14]. Large armchair (zigzag) nanotubes, with diameter of about 40 Å (53 Å), behave like graphene (and this is quite logic due to the low curvature of the cylinders). For small nanotubes however the 5|8|5 defect is instead *most stable* than the (555-777)one and the zigzag chirality plays again against the (555-777) defect when CNT's with small diameter are considered. Analogous results are reported for graphene finite sized portions (graphene flakes) in the recent article [16].

The G_{888} lattice presents, after the first SW, the (555-777) morphology given in Figure 2b. The octagon has disappeared replaced by a more complex structure with a three-fold configuration that includes three fused heptagons plus three satellite pentagons. The graph $G_{888-777}$ is characterized by the new invariants $\rho^E(G_{888-777}) = 1.06498952$ and W($G_{888-777}$) =23514. In this case then the topological potential Ξ^{ρ^E} plays against the SW rotation that causes the passage from G_{888} to lattice $G_{888-777}$.Both defects are present in graphene layers and reversible $G_{888} \leftrightarrow G_{888-777}$ switching is also reported [9].

A second SW rotation may take place acting on the bond shared by one of the heptagons and the external hexagon, indicated with the arrow in Figure 2b;in this way the lattice assumes a novel "quadrupolar" structure named (5555-6-7777) defect. In literature, the formation energy of this quadrupolar defect has been found between those of 5|8|5and (555-777) [9] whereas other DFT calculations consider [13]the difference in the formation energy between the two defective configurations (5555-6-7777)and (555-777)quite small of the order of ~0.1 eV. Figure 2c represents the periodic super-cell of the $G_{8888-6-7777}$ graph having topological roundness of $\rho^E(G_{8888-6-7777}) = 1.02801856$ and W($G_{8888-6-7777}$) =23482.

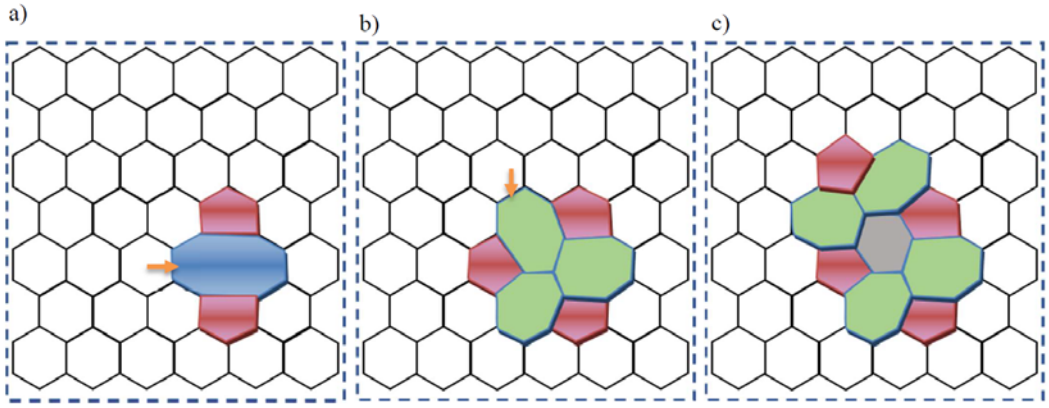

Figure 2. a) The G_{585} lattice; the arrowed bond allows a SW rotation that produces defect (555-777) represented in b). By rotating the bond indicated with the arrow in b) the (5555-6-7777) quadrupolar configuration is produced c). Rings colored in red, green, blue, rings have 5,7,8 carbon atoms respectively. Hexagons are colored in white and gray.

Figure 3 summarizes the behaviors of the topological potential $\Xi^{\rho^{E}} - \rho^{E}$ in the various passages that transform the pristine graphene lattice G_0in the final divacancy graphene with the quadrupolar structure$G_{5555-6-7777}$.

The first part of the curve shows the response of the topological potential to the creation of a single vacancy SV and then to the introduction of the second vacancy DV that allows the generation of the 5|8|5 rearrangement in the graphene lattice. The creation of the single vacancy SV breaks the perfect symmetry of the periodic graphene super-cell $G_0$by creating a three-fold "crater" in the honeycomb mesh increasing the value of the topological potential$\Xi^{\rho^{E}}$. The introduction of the second vacancy is obtained by eliminating one of the 3 atoms that SV leaves with one dandling bond, with the creation of a symmetric DV hole with two mirror planes. The topological potential$\Xi^{\rho^{E}}$ (DV) does not therefore vary too much in respect to $\Xi^{\rho^{E}}$ (SV) confirming the results obtained by ab-initio simulations [9] that indicate that the formation energy of DV is close to the SV one, about 8 eV. The topological model predicts the evolution of the DV lattice toward the 5|8|5 configuration whose increased stability is signaled by the $\Xi^{\rho^{E}}$ reduction (see Figure 3). The topological model fails, when compared with the results of ab-initio simulations (see previous section) in predicting the passage from the G_{585} lattice to the defective graph (555-777) represented in Figure1a,1b. The topological efficiency is larger for the (555-777) and from the topological point of view the systems therefore privileges the 5|8|5 configuration. Finally, the quadrupolar structure $G_{5555-6-7777}$ presents a topological stability in terms of $\Xi^{\rho^{E}}$ that is comparable with the one of the G_{585} lattice. This last result confirms the study [9] in which the authors state that the formation energy of the (5555-6-7777) defective lattice "is between those of 5|8|5 and (555-777)".

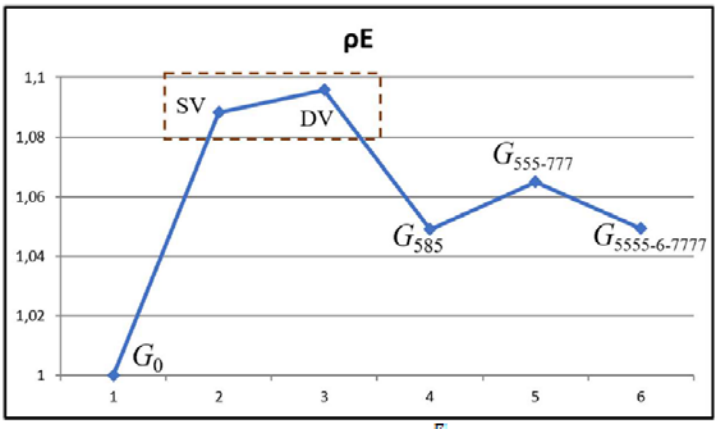

Figure 3. The curve of the topological roundness $\Xi^{\rho^E} - \rho^E$ is given for the various defective lattices that are created starring from the pristine graphene super cell G_0 with the introduction of a single vacancy SV and a double vacancy DV.

Figure 3 shows that, ranked by Ξ^{ρ^E}, the 3 competing lattices with a DV show the stability sequence 5|8|5, (5555-6-7777) and (555-777). This result is compatible with the TEM observed transitions [18] among defective configurations $G_{585} \leftrightarrow G_{555\text{-}777} \leftrightarrow G_{5555\text{-}6\text{-}7777}$.

Once more, our study points out the *somehow surprising* ability of the topological roundness to simulate, in a negligible amount of CPU time, the physical behavior of complex sp^2 carbon systems. The method gets boosted by the natural (and computationally easy way) the topological invariants have for taking into consideration long-range interactions between all pairs of atoms in large nanostructures.

4. CONCLUSIONS

The simulations of defective graphenic lattices based on topological potentials like the topological roundness produce interesting answers concerning relative stability lattices with a divacancy, predicting an apparent predominance of the pentagon-octagon-pentagon defect, followed by the quadrupolar DV rearrangement.

Therefore, further insight by determination of energetic and thermodynamic quantities with observable character are needed, including the combination of the present topological approach with the "bondon" quasi-particle picture, an innovative physical entity corresponding to the quantum particle of the chemical bond [17], recently applied to investigate influence of topological long-range interaction on the properties of one-dimensional graphenic nanoribbons [18]. In such a picture the stability of a defective structure will be judged in terms of bondonic life-time for "covering" the super-cell of the system that is associate to the characteristic bondonic frequency; it also provides the route for the spectroscopic detection of the bondonic states through Raman, Compton or allied solid state techniques.

Our results shed new light on the fundamental processes that dominate the rearrangement of carbon networks, and the processes that we investigate in this study are likely be replicated in the formation of other carbon nanostructures from carbon vapor, such as nanotubes and fullerenes. Moreover, present topological investigations are worth to be extended to non sp^2

systems like the black phosphorus that is currently targeted by many experimental investigations and detailed ab-initio theoretical studies [19] dealing with the role of SW rotation and SV and DV in creating defects in black phosphorus motivating further topological investigations in the area of material with tunable band-gaps and magnetic fictionalization.

REFERENCES

[1] Geim, A.K., 2009. Graphene: status and prospects. science, 324(5934), pp.1530-1534.

[2] Jariwala, D., Sangwan, V.K., Lauhon, L.J., Marks, T.J. and Hersam, M.C., 2013. Carbon nanomaterials for electronics, optoelectronics, photovoltaics, and sensing. Chemical Society Reviews, 42(7), pp.2824-2860.

[3] Zhang, Y., Tan, Y.W., Stormer, H.L. and Kim, P., 2005. Experimental observation of the quantum Hall effect and Berry's phase in graphene. Nature, 438(7065), p.201-204.

[4] Putz, M.V. and Ori, O., 2014. Bondonic effects in group-IV honeycomb nanoribbons with Stone-Wales topological defects. Molecules, 19(4), pp.4157-4188.

[5] Koorepazan-Moftakhar, F., O. Ori O. & Ashrafi,A.R.(2018) Symmetry − Based Invariants of Nanostructures and Their Effect on Edge States of Carbon Nanotubes, Fullerenes, Nanotubes and Carbon Nanostructures, DOI: 10.1080/1536383X.2018.1558402

[6] Bultheel, A. and Ori, O., 2018. Topological modeling of 1-Pentagon carbon nanocones–topological efficiency and magic sizes. Fullerenes, Nanotubes and Carbon Nanostructures, 26(5), pp.291-302.

[7] Ori, O. & Putz, M. V. (2014) Isomeric Formation of 5|8|5 Defects in Graphenic Systems, Fullerenes, Nanotubes and Carbon Nanostructures, 22:10, 887-900,

[8] L. Liu et al. "Defects in Graphene: Generation, Healing, and Their Effects on the Properties of Graphene: A Review" Journal of Materials Science & Technology 31 (2015) 599-606

[9] Banhart, F., Kotakoski, J. and Krasheninnikov, A.V., 2010. Structural defects in graphene. ACS nano, 5(1), pp.26-41.

[10] Dunk, P.W., Kaiser, N.K., Hendrickson, C.L., Quinn, J.P., Ewels, C.P., Nakanishi, Y., Sasaki, Y., Shinohara, H., Marshall, A.G. and Kroto, H.W., 2012. Closed network growth of fullerenes. Nature communications, 3, p.855.

[11] Putz, M.V. and Ori, O., 2012. Bondonic characterization of extended nanosystems: Application to graphene's nanoribbons. Chemical Physics Letters, 548, pp.95-100.

[12] Iranmanesh, A., Ashrafi, A.R., Graovac, A., Cataldo, F., and Ori, O. (2012) Wiener index role in topological modeling of hexagonal systems - from fullerenes to grapheme. In

Distance in Molecular Graphs – Applications; Gutman, I and Furtula, B. (eds.), Univ. Kragujevac: Kragujevac, pp. 135–155.

[13] Chen, Q., Robertson, A.W., He, K., Gong, C., Yoon, E., Lee, G.D. and Warner, J.H., 2015. Atomic Level Distributed Strain within Graphene Divacancies from Bond Rotations. ACS nano, 9(8), pp.8599-8608.

[14] Amorim, R.G., Fazzio, A., Antonelli, A., Novaes, F.D. and da Silva, A.J., 2007. Divacancies in graphene and carbon nanotubes. Nano Letters, 7(8), pp.2459-2462.

[15] Lherbier, A., Dubois, S.M.M., Declerck, X., Roche, S., Niquet, Y.M. and Charlier, J.C., 2011. Two-dimensional graphene with structural defects: elastic mean free path, minimum conductivity, and Anderson transition. Physical review letters, 106(4), p.046803.

[16] Liu, L. and Chen, S., 2017. Geometries and Electronic States of Divacancy Defect in Finite-Size Hexagonal Graphene Flakes. Journal of Chemistry, 2017.

[17] Girit, Ç.Ö., Meyer, J.C., Erni, R., Rossell, M.D., Kisielowski, C., Yang, L., Park, C.H., Crommie, M.F., Cohen, M.L., Louie, S.G. and Zettl, A., 2009. Graphene at the edge: stability and dynamics. science, 323(5922), pp.1705-1708.

[18] Kotakoski, J.; Krasheninnikov, A. V.; Kaiser, U.; Meyer, J. C. From Point Defects in Graphene to Two-Dimensional Amorphous Carbon. Phys. Rev. Lett. 2011, 106, 105505.

[19] Gaberle, J. and Shluger, A.L., 2018. Structure and properties of intrinsic and extrinsic defects in black phosphorus. Nanoscale, 10(41), pp.19536-19546.